Liquid Crystals
Publication details, including instructions for authors and subscription information:
http://www.informaworld.com/smpp/title~content=t713926090

Structure-property relationships of 'diluted' ferroelectric polysiloxanes

Holger Poths[a]; Rudolf Zentel[a]
[a] Institut für Organische Chemie, Universität Mainz, Mainz, Germany

To cite this Article Poths, Holger and Zentel, Rudolf(1994) 'Structure-property relationships of 'diluted' ferroelectric polysiloxanes', Liquid Crystals, 16: 5, 749 — 767
To link to this Article: DOI: 10.1080/02678299408027848
URL: http://dx.doi.org/10.1080/02678299408027848

LIQUID CRYSTALS, 1994, VOL. 16, NO. 5, 749–767

Structure–property relationships of 'diluted' ferroelectric polysiloxanes

by HOLGER POTHS and RUDOLF ZENTEL*
Institut für Organische Chemie, Universität Mainz,
J. J.-Becherweg 18-20, 55099 Mainz, Germany

(*Received 14 June 1993; accepted 6 July 1993*)

A series of new ferroelectric copolysiloxanes with systematically varied comonomer content ('dilution') has been synthesized. Good planar alignment could be achieved for all copolysiloxanes and they were studied with respect to their mesomorphic and ferroelectric properties. Broad enantiotropic S_C^* phases and spontaneous polarizations up to 286 nC cm^{-2} are found. X-ray diffraction experiments show a linear increase of the smectic layer spacing by 'dilution'. This points to a microphase separated structure of mesogenic groups and siloxane chains. It is found that the fixation of a mesogen to homopolysiloxane leads to an increase of P_S, whereas the 'dilution' of the mesogens with dimethylsiloxane units decreases P_S again. Based on the microphase separated model, it can be shown that the decrease of P_S is not only due to the decrease of the vol % of mesogenic groups. The coupling between different mesogens mediated by the polymer chain, has additionally to be taken into consideration. A remarkable drop in the response times τ with decreasing mesogen content is confirmed and switching times less than 1 ms were measured.

1. Introduction

Low molecular weight ferroelectric liquid crystals (LMWFLC) have been widely investigated in recent years, because of their potential for fast switching and their memory effect in displays [1–3]. Since 1984, liquid crystalline polymers with chiral smectic C* phases [4–12] have been prepared and their ferroelectric properties determined. This allows the combination of typical polymeric features with the properties of the ferroelectric S_C^* state. Thus, ferroelectric polymers offer the possibility of introducing additional functional groups like dyes [13, 14], NLO-chromophores [9] and crosslinkable groups [15–17] into ferroelectric phase. Therefore new applications such as, for example, piezoelements from crosslinked S_C^* elastomers [15–17] might be possible.

Through the fixation of the mesogenic cores to a polymer backbone, the phase transition temperatures are increased and due to their higher viscosity, slower response times τ than in LMWFLC are obtained. In this regard, FLC polymers, especially those containing polysiloxane [6, 8, 9] backbones were synthesized, because the low glass transition temperature of the polysiloxane backbone [18] ($T_g \approx -123$°C) and the low viscosity give rise to moderate phase transitions and shorter switching times. By the preparation of copolysiloxanes, in which only a part of the monomer units are functionalized with mesogenic groups ('diluted' polysiloxanes from poly-(methylhydrogen-co-dimethyl)-siloxanes), a further reduction of T_g can be obtained. These 'diluted' copolysiloxanes show response times in the submillisecond region [19, 20]. Due to their low viscosity they can be processed into free standing films [21].

* Author for correspondence.

Apart from these investigations on 'diluted' polysiloxanes, no effort has been made until now, to correlate the properties of the polymers (for example, phase width, spontaneous polarization P_S, response time τ) with the special structure of the liquid crystalline phase in these polymers.

We present here a detailed description of the synthesis and characterization of 'diluted' ferroelectric polysiloxanes, which can give an explanation for the phase behaviour and the ferroelectric properties depending on their molecular structure.

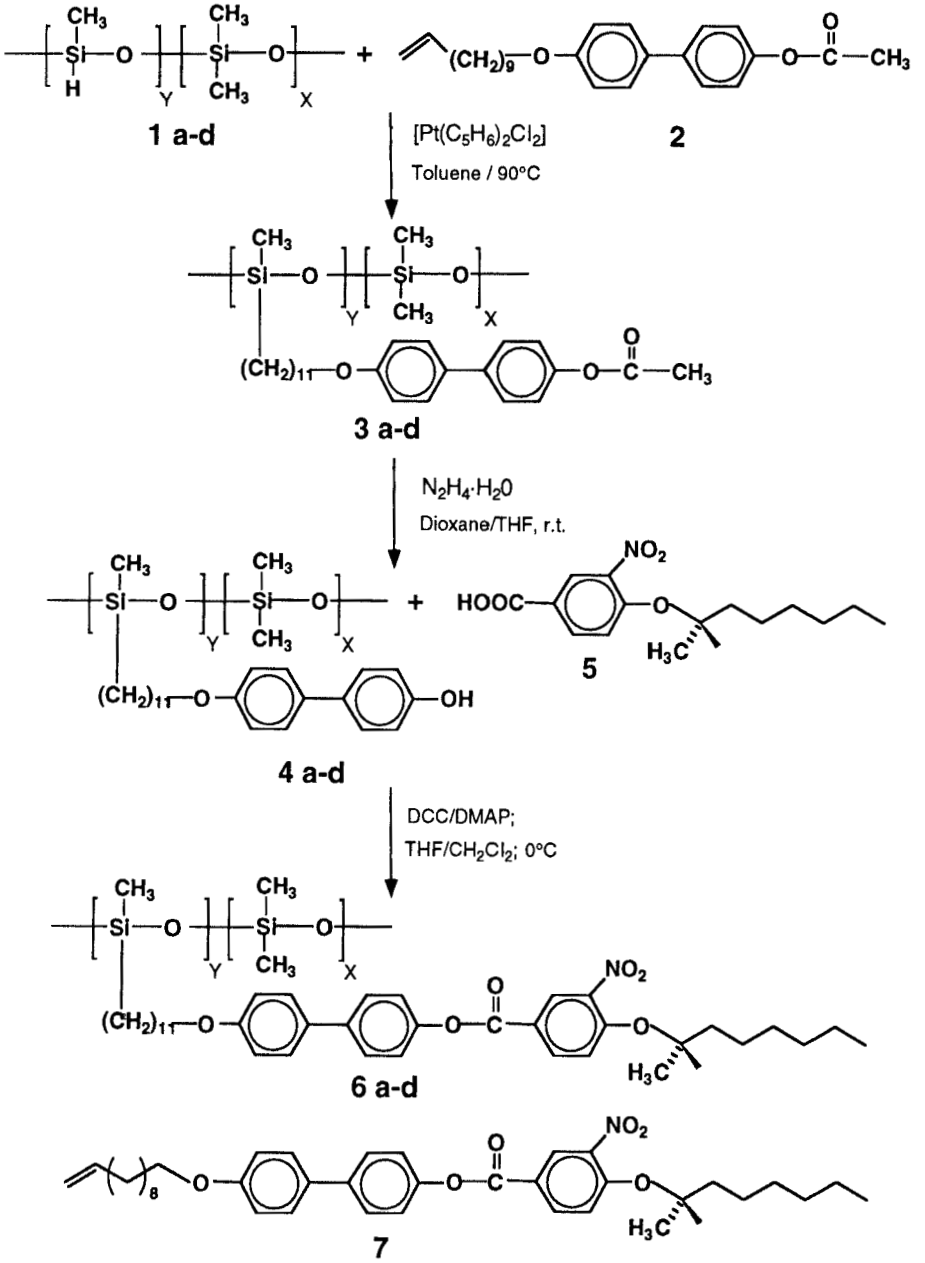

Scheme.

2. Synthesis and characterization

The structures and the synthetic route to the ferroelectric polysiloxanes **6a–d** are given in the scheme. Starting with a classical hydrosilylation [22–24] of poly-(methylhydrogen-co-dimethyl)-siloxane ($P_n > 30$) and poly-(methylhydrogen)-siloxane ($P_n = 35$) **1a–d** with 4-(undec-10-enyloxy)-4′-acetoxybiphenyl [9] **2** in toluene under $[Pt(C_{10}H_{12})Cl_2]$ [25] catalysis leads to the polysiloxanes **3a–d** with a pendent acetate protecting group. For polymer **3d**, not all Si–H groups could be hydrosilylated with the mesogenic side chain **2**. They were removed with a 10-fold excess of 1-octene, so that in **3d** some octyl groups (< 15 per cent) were detected by NMR. For further discussions the octylgroups in this polymer were treated like conventional dimethylsiloxane units, because they are chemically similar. Compounds **3a–d** exhibit smectic polymorphism (see table 1).

In the next step, all the acetate protecting groups were cleaved by hydrazinolysis in THF/dioxane, resulting in the crystalline polysiloxanes **4a–d** (see table 1). Their phenolic hydroxy groups could be quantitively esterified with 3-nitro-4-(1-(*S*)-methylheptyloxy) benzoic acid **5** in the presence of *N*,*N*′-dicyclohexylcarbodiimide (DCC) and 4-*N*,*N*-dimethylaminopyridine (DMAP) by a polymer analogous reaction to give the ferroelectric polysiloxanes **6a–d**. We adopted this polymer analogous esterification a few years ago for chiral combined LC polymers [26, 27], chiral polyacrylates [28] and ferroelectric homopolysiloxanes [9, 29]. ^{1}H NMR measurements confirm that all hydroxy groups were esterified by the chiral acids within the limits of accuracy (> 95 per cent) [26, 27]. The low molar mass liquid crystal (monomer) **7** was synthesized analogously for comparison. The phase assignment of the polysiloxanes **6a–d** (see figure 2) was done on the basis of polarizing microscopy using an Ortholux II-Pol-BK (Leitz) microscope equipped with a Mettler FP 52 hot stage. DSC measurements were recorded using Perkin–Elmer DSC-2C and DSC 7 instruments with a heating or cooling rate of $\pm 10°C\,min^{-1}$. Peak maxima of the second heating were taken for the determination of the phase transitions. Temperature-dependent X-ray measurements of powder samples were performed with a Siemens TT 500-Goniometer equipped with a home-made vacuum oven. The molecular weights were determined by analytical GPC against polystyrene standards.

Table 1. Phase transitions and molecular weights of polymers **3a–d** and **4a–d**.

Polymers (copolymerization ratio)	Phase transition/°C†							Molecular weight‡	
	T_g	C	S_X		S_A		I	M_w	M_n
3a ($X = 0$, $Y = 1$)	42	123	•	152	•	186	•	21 000	13 000
3b ($X = 0{\cdot}5$, $Y = 1$)	34	113	•	144	•	171	•	44 000	21 000
3c ($X = 1{\cdot}1$, $Y = 1$)	27	104	•	124	•	140	•	47 000	18 000
3d ($X = 3{\cdot}2$, $Y = 1$)	3	96§			•	109§	•	17 000	9000
4a ($X = 0$, $Y = 1$)		190					•	13 000	9000
4b ($X = 0{\cdot}5$, $Y = 1$)		175					•	30 000	21 000
4c ($X = 1{\cdot}1$, $Y = 1$)		150					•	36 000	17 000
4d ($X = 3{\cdot}2$, $Y = 1$)		141					•	18 000	11 000

† C: crystalline, T_g: glass transition temperature, S_X: higher ordered smectic phase, S_A: smectic A phase, I: isotropic.

‡ GPC in $CHCl_3$ for **3a–d** and in THF for **4a–d**.

§ Overlapping transitions.

Table 2. Phase transitions, spontaneous polarization P_s, tilt Θ, response time τ and molecular weights of polymers **6a–d** and LWMFLC **7**.

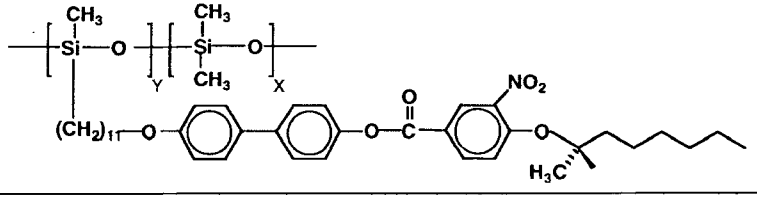

Polymers (copolymerization ratio)	Phase transition temperatures/°C†									Physical properties			Molecular weight	
	T_g	S_X		S_C		S_A		I		P_s/nC/cm^2‡	Tilt Θ/°‡	τ/ms§	M_w	M_n
6a ($X=0$, $Y=1$)	21	•	57	•	156	•	183	•		211	29	17·3	28 000	13 000
6b ($X=0{\cdot}5$, $Y=1$)	20	•	72	•	138	•	182	•		161	26	2·6	51 000	29 000
6c ($X=1{\cdot}1$, $Y=1$)	13	•	54	•	124	•	168	•		130	27	1·6	53 000	27 000
6d ($X=3{\cdot}2$, $Y=1$)	0	•	46	•	98	•	144	•		104	26	3·9	23 000	14 000
7 (LMWFLC)		•	61¶	•	80	•	88	•		184	27	0·1		

†T_g: glass transition temperature; S_X: higher ordered smectic phase; S_C^* chiral smectic C* phase; S_A: smectic A phase; I: isotropic.
‡All values taken at $T_c - T = 10°C$; $T_c = S_C^*$–S_A^* transition temperature.
§Applied field: $10\,V_{pp}\,\mu m^{-1}$, taken at $T_c - T = 10°C$.
¶Crystalline–S_C^* transition.

(*a*)

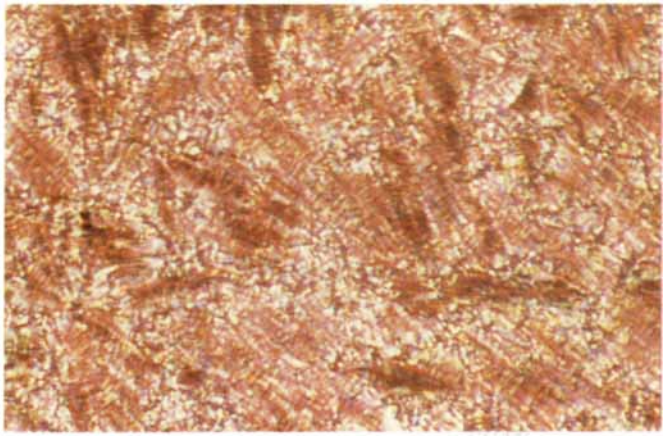

(*b*)

Figure 1. Optical photomicrographs of the textures of polymer **6c**. (*a*) S_A phase (127°C); (*b*) S_C^* phase (121°C). Magnification × 378.

(*a*)

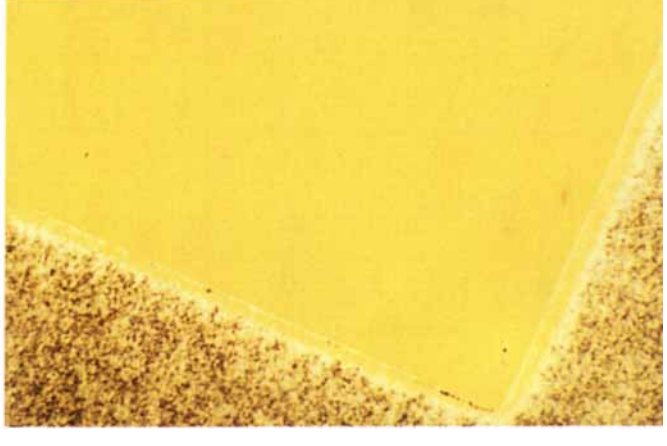

(*b*)

Figure 6. The two switched states of the ferroelectric polysiloxane **6d** between crossed polarizers in a 4 μm EHC-cell at $T = 88$°C. The dark state corresponds to the director of one switched state lying along the optical polarization direction. Magnification × 96.

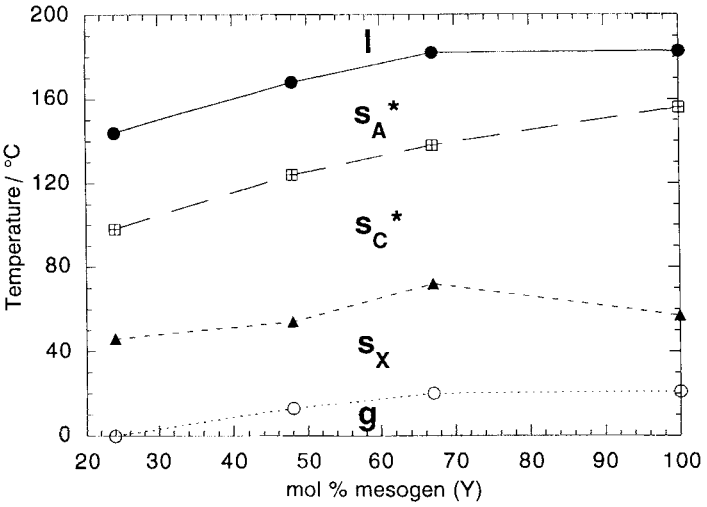

Figure 2. Phase diagram for the copolysiloxanes **6a–d**. Phase transition temperatures as a function of mol% of mesogen.

On slowly cooling from the isotropic phase into the LC phase, typical fan-shaped textures of a S_A phase (see figure 1 (*a*)) could be observed for all polysiloxanes **6a–d**. On further cooling the chiral smectic C* phase appeared as broken fan-shaped textures (see figure 1 (*b*)). The S_C^*–S_A^* transition could not be detected by DSC for the 'diluted' polysiloxanes **6d–d**, but was observed by polarizing microscopy. Below the S_C^* phase, a higher ordered smectic phase (S_X) was confirmed by DSC and X-ray measurements. All data are compiled in table 2.

In figure 2 the phase transition temperatures for polymer **6a–d** are plotted against the substitution level of mesogenic groups (in mol%). It is interesting to note that even up to a high degree of 'dilution', the LC phases are retained and broad enantiotropic S_C^* and S_A^* phases are found. On 'dilution' (= decreasing mesogen content Y), the S_A^* phase is broadened relatively to the S_C^* phase. Furthermore the glass transition temperatures are lowered by about 20°C. Since the clearing temperatures are more strongly decreased ($\approx$40°C), an overall phase destabilization results.

3. Structural investigations of 'diluted' ferroelectric polysiloxanes

Temperature-dependent X-ray diffraction patterns were obtained for powder samples of polysiloxanes **6a–d**. The diffraction for **6a**, which is typical for all the investigated systems is displayed in figure 3. In the S_C^* phase ($T = 142$°C), the spectrum is dominated in the small angle region by well-pronounced Bragg peaks (up to the fifth order), indicating a well-established smectic layer structure, which is different from the sinusoidal density modulation of low molar mass smectic materials. In the wide angle region ($2\Theta \approx 19{\cdot}8°$), only a broad diffuse halo is observed, which is characteristic for a fluid analogue packing of the mesogens within each smectic layer of a S_C^* phase. The 002 reflection (32·1 Å) corresponds to the length of a tilted monolayer, whereas the 001 reflection (bilayer) could not be resolved with the set-up used, but its existence was confirmed by electron diffraction [30]. In the S_A phase the layer spacings are slightly increased $\approx$1·3–1·5 Å in comparison to the S_C^* phase. Calculating the tilt angle from X-ray measurements yields only 60 per cent of the value determined from optical Θ-measurements. This may be due to a change in the extent of interdigitation of the side

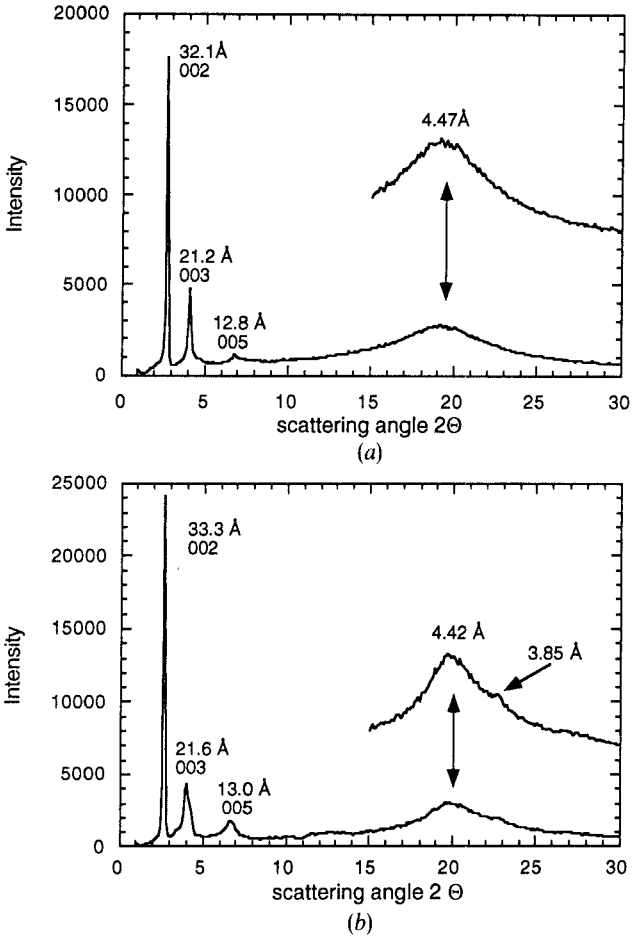

Figure 3. Temperature-dependent X-ray powder diffractograms for **6a**. (*a*) $T = 142°C$, S_C phase and (*b*) $T = 23°C$, S_X phase.

chains and/or the zig–zag arrangement [31] of the mesogens. By cooling the sample into the S_X phase, only a small shift in the smectic layer distances is observed, whereas the half-width of the halo is reduced and it splits up (additional reflection at 3·85 Å). The appearance of an additional reflection corresponds to an ordering of the mesogens within the smectic layer, which is typical for a higher ordered phase.

Apart from the characterization of the smectic phases, we were interested in the influence of the 'dilution' on the smectic layer structure. For this reason, we have plotted the smectic layer spacings (002 reflection) in the S_C^* phase (reduced temperature $T_c - T = 10°C$) as a function of the ratio of inserted dimethylsiloxane units to mesogenic siloxane units ($= X$) in figure 4. A linear relationship of the layer spacings d_{total} on the 'dilution' is observed following equation.

$$d_{total} = d_{mesogen} + d_{siloxane} = d_{mesogen} + \text{const.} \cdot X, \quad (1)$$

where X is the ratio of inserted dimethylsiloxane units to mesogenic siloxane units. This result can be explained on the basis of a microphase separation first described by Diele [32–34], which suggests that the siloxane chains are segregated from the mesogens due to immiscibility. They are supposed to form a siloxane sublayer, which is separated from a sublayer of smectic mesogens (see figure 5). For this model, the

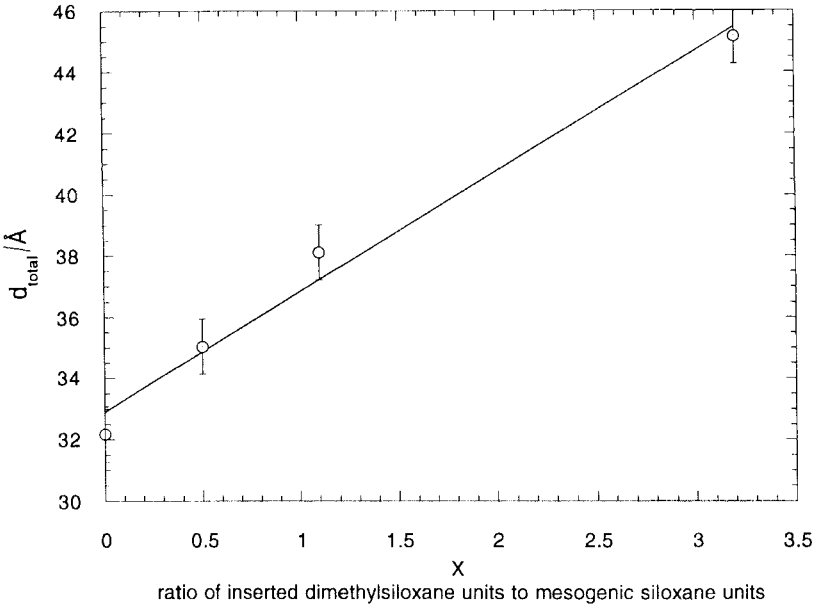

Figure 4. Layer spacings d_{total} as a function of the ratio of inserted dimethylsiloxane units to mesogenic siloxane units (X) for $T_c - T = 10°C$.

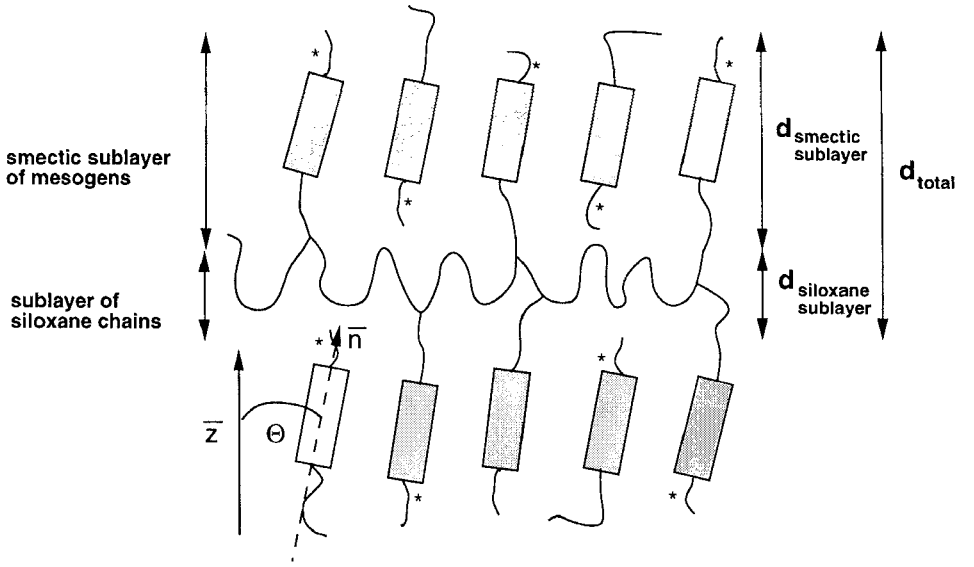

Figure 5. Schematic of a microphase separated structure of a 'diluted' polysiloxane in the S_C^* phase. The siloxane chains are segregated from the mesogens due to immiscibility forming two sublayers with a thickness of $d_{mesogen}$ and $d_{siloxane}$. The layer spacing d_{total} is the sum of $d_{mesogen}$ and $d_{siloxane}$.

measured d_{total} values are the sum of both increments, of the siloxane sublayer ($d_{siloxane}$) and the sublayer of the mesogens ($d_{mesogen}$). Due to the microphase separation, only the siloxane sublayer becomes swollen by 'dilution' without affecting the sublayer of mesogenic groups. From this model, it is obvious that the LC phases of the ferroelectric polysiloxanes **6a–d** are retained up to high degrees of 'dilution' (see figure 2), because the increase in the number of dimethylsiloxane units ('dilution') swells the siloxane sublayer, but it does not disturb the mesogenic interactions within the smectic sublayer too much. At this point it is important to mention that this microphase separation happens only on the level of the smectic layers and no macrophase separation could be observed, for example, by microscopy.

4. Ferroelectric properties

The electro-optical measurements were performed using 10 μm commercially available LC-cells (EHC, Japan). The cells were filled with the polymers in the isotropic phase on a Kofler hot bench by capillary forces. Good planar alignment (see figure 6) was achieved by repeated heating and cooling of the samples from the S_A^* to the S_C^* phase while applying an AC field ($f = 3$ Hz) of 100 V_{pp}. The spontaneous polarization P_S was measured according to the triangular wave method [35, 36]. The polarization current was measured as a voltage drop across a series resistance of 10 kΩ with a Hewlett–Packard HP 54601A digital storage oscilloscope. The data were read into a computer and ohmic and capacitive contributions were separated and integrated by the computer. Usually a 3–10 $V_{pp}\,\mu m^{-1}$ amplitude triangular wave ($f = 10$–1 Hz) was sufficient to obtain saturation of the polarization. P_S values for the polymer **6a–d** were measured on cooling from the S_A^* phase, because sometimes a certain hysteresis effect (20–30 per cent) was observed on comparing heating and cooling cycles. The electro-optic switching times τ were determined with a photodiode measuring the transmitted light intensity of the sample between crossed polarizers. The switching time τ is defined here as the time required for an intensity change from 0–100 per cent on applying a square wave ($f < 1$ Hz). Tilt angle measurements were made under quasi DC conditions ($f < 0{\cdot}4$ Hz) using the difference in angular readings on the microscope turntable for two nearby transmission minima giving the full smectic C cone angle, or twice the tilt angle.

A typical oscilloscope trace for polymer **6d** at $T = 83$°C (S_C^* phase) showing the polarization current peaks with a low ionic conductivity and their coincidence with the fast change in the optical transmission is displayed in figure 7.

The temperature dependence of the spontaneous polarization was determined for all polymers and some values are collected for a given reduced temperature of $T_c - T = 10$°C in table 2. The highest P_s value that we have measured is 286 nC cm^{-2} at 97°C for the homopolymer **6a**. Looking at the temperature dependence of polysiloxane **6d** (figure 8), P_S reaches a maximum value of 139 nC cm^{-2} at 60°C. No measurements could be made below this temperature because of its large viscosity, although a bistable switching could be observed even at lower temperatures. Close to the S_C^*–S_A^* transition a voltage dependence of the spontaneous polarization is observed. For small electrical fields (3–5 $V_{pp}\,\mu m^{-1}$), P_S goes continuously to zero at the transition from the ferro- to the paraelectric phase indicating the second order nature of the transition. In contrast to this, at higher applied fields (15–20 $V_{pp}\,\mu m^{-1}$) a spontaneous polarization could also be measured well above the phase transition in the S_A^* phase.

In figure 9 oscilloscope traces for polymer **6d** at 102°C ($T - T_c = 4$°C) in the S_A^* phase are recorded as a function of the applied field. Applying a low AC field, an

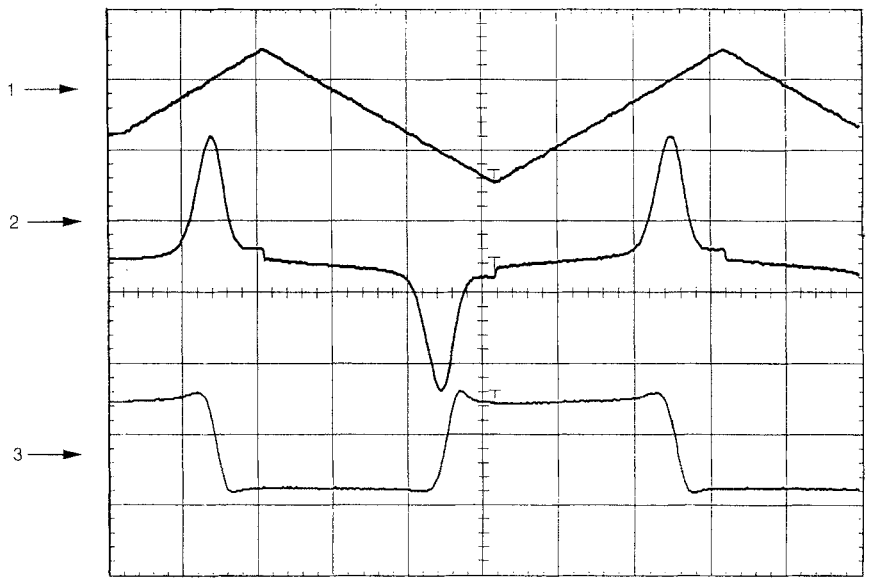

Figure 7. Oscilloscope trace of the ferroelectric switching of polymer **6d** in a 4 μm EHC cell at $T = 83°C$. **1**: applied voltage, 38 V_{pp}, $f = 3{\cdot}2$ Hz; **2**: current response as a voltage drop across $R_s = 10\,k\Omega$, $P_s = 114\,nC\,cm^{-2}$; optical response from the photodiode.

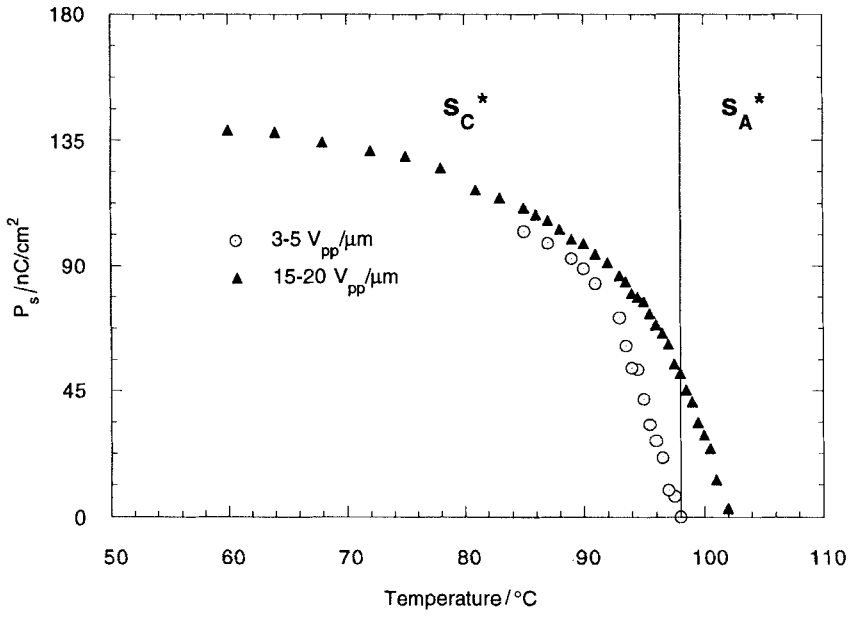

Figure 8. Temperature dependence of the spontaneous polarization P_s for polymer **6d** (10 μm EHC cell) for E fields of 3–5 $V_{pp}\,\mu m^{-1}$ and 15–20 $V_{pp}\,\mu m^{-1}$.

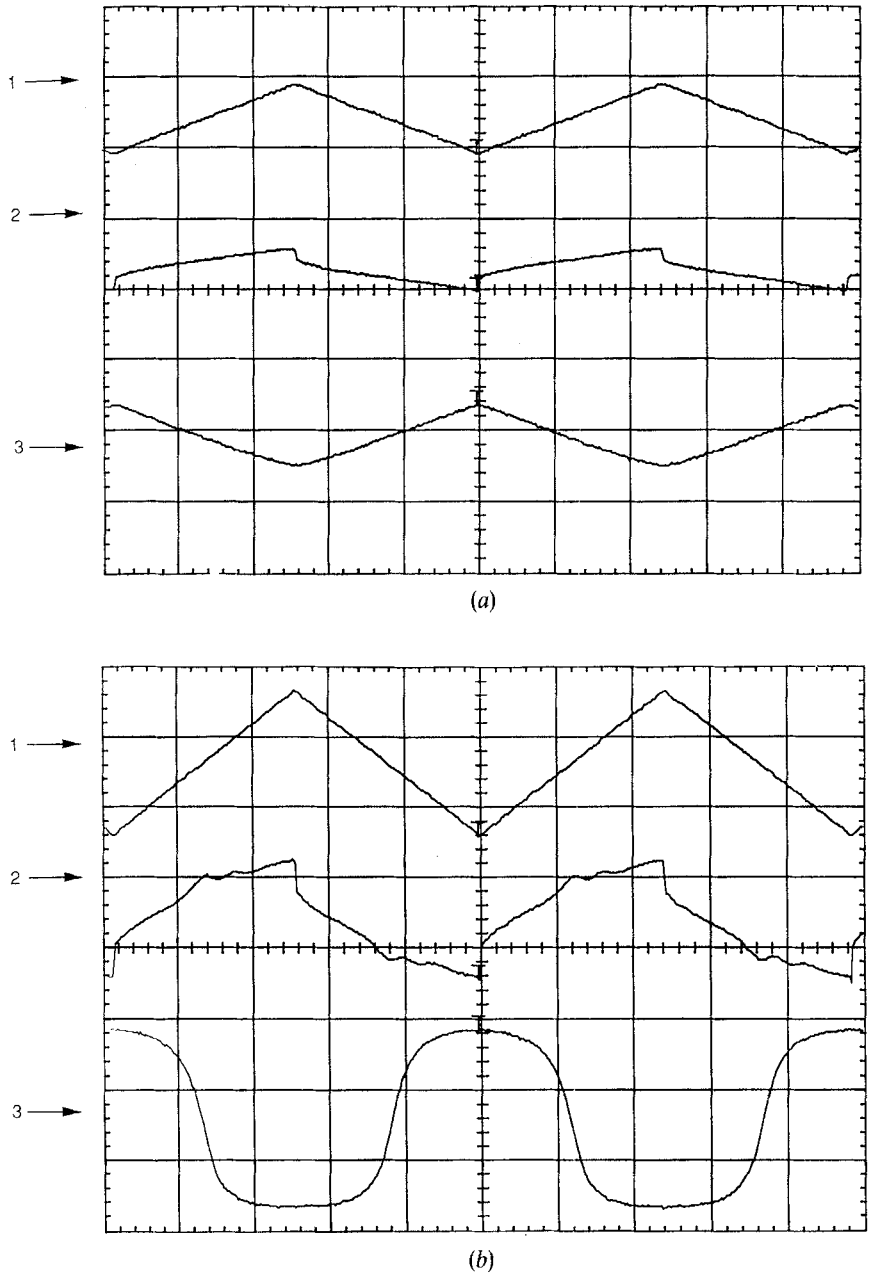

Figure 9. Oscilloscope traces of the switching behaviour of polymer **6d** at 102°C in a shear cell (3 μm). (*a*) **1**: applied voltage 10 V_{pp}; **2**: current response as a voltage drop across R_S = 20 kΩ; **3**: optical response from the photodiode; (*b*) **1**: applied voltage 100 V_{pp}; **2**: current response as a voltage drop across R_S = 20 kΩ; **3**: optical response from the photodiode.

electroclinic switching (see figure 9 (*a*)) is observed with the photodiode, whereas at high fields (20–25 $V_{pp}\,\mu m^{-1}$), a drastic change from an electroclinic to a bistable optical response (see figure 9 (*b*)), which is characteristic for a S_C^* phase, is observed. This effect looks, at first, like a shift in the phase transition temperatures to higher temperatures (phase induction). The correct interpretation may however be different. *E* fields induce in the smectic A phase, close to the S_C^* phase, large tilt angles of the mesogenic groups (electroclinic effect). For polymer **6d**, Θ_{ind} of $\approx 20°$ were measured at 102°C with $25\,V_{pp}\,\mu m^{-1}$ [37]. This should lead to a large induced polarization. On reversing the sign of the *E* field, two switching mechanisms are possible. First a normal soft-mode behaviour (electroclinic, no P_S detectable) and secondly a cone switching, driven by the interaction of the external *E* field and the induced polarization P_{ind} of the tilted arrangement. For large induced tilt angles and high external fields, this cone switching ($\tau \sim [E \cdot P_{ind}]^{-1}$) can be faster than the electronic switching (τ independent of *E*) or, in other words, the cone switching may be finished before the tilted smectic structure has time to relax completely. As a consequence, a mixed electroclinic/cone switching with detectable P_S can result.

At higher temperatures ($T - T_c = 22°C$), a pure electroclinic switching with induced tilt angles $\Theta_{ind} \approx 5°$, in combination with a high soft-mode frequency of 15 kHz, is found [37].

In order to investigate the influence of the 'dilution' on the spontaneous polarization for the polymers **6a–d**, we have plotted (see figures 10 and 11) P_S as a function of the substitution level of the siloxane backbone modified with mesogenic side chains (mol % and vol % of mesogens). A strong decrease of P_S is observed ranging from $104\,nC\,cm^{-2}$ for the most 'diluted' polymer **6d** up to $211\,nC\,cm^{-2}$ for the homopolymer **6a** is found (see table 2). For the monomer **7**, a P_S of $184\,nC\,cm^{-2}$ is found, which is smaller than the P_S of the homopolymer **6a**. Since only a slight variation of the tilt angles Θ was measured for **6a–d** and **7** (see table 2), this obviously cannot be

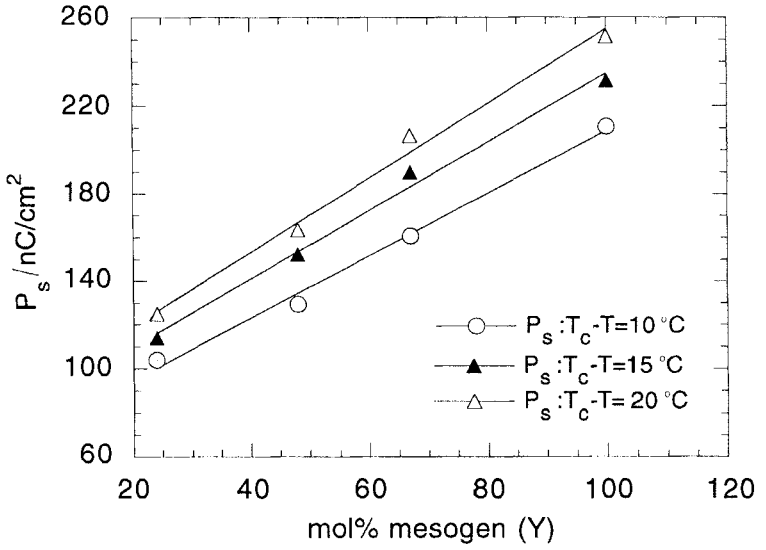

Figure 10. Spontaneous polarization P_s of polymers **6a–d** versus mol % of mesogen (*Y*) for $T_c - T = 10°$, 15° and 20°C.

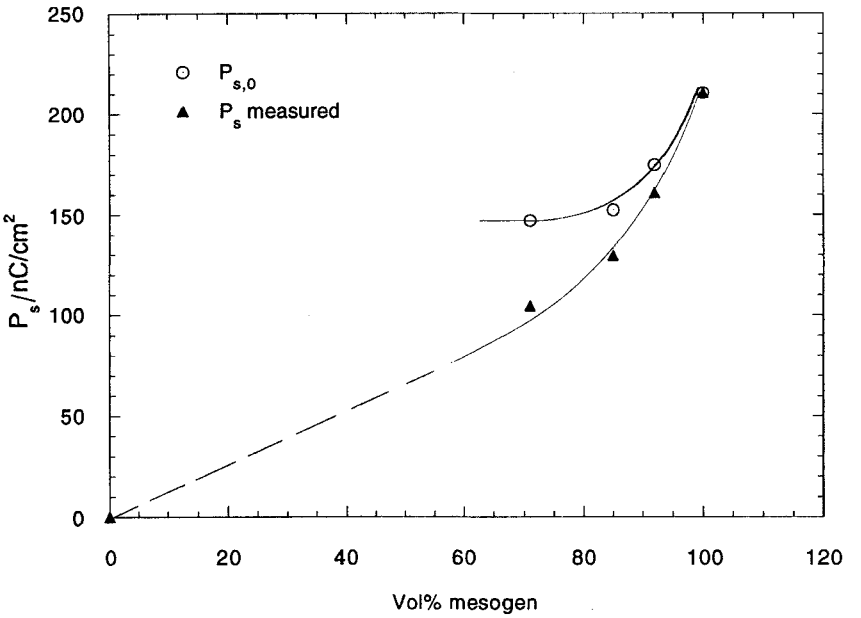

Figure 11. P_s and $P_{s,0}$ as a function of vol% of mesogen for polysiloxanes **6a–d** at $T_c - T = 10°C$. $P_{s,0}$ is the polarization of the material, if it were composed of 100 vol% mesogenic sublayers. The solid line is a guide to the eye.

the reason for the large differences in the P_S values. A linear dependence of P_S on the volume ratio of mesogens (vol% mesogens; defined by equation (2)) would be expected from the microphase separated model (figure 5 and equation (1)). Since the 'dilution' swells only the siloxane compartment, its thickness increases linearly in relation to the mesogen compartment. Assuming a constant polarization per sublayer of mesogens, this would lead to a linear decrease in the polarization (see equation (3)) with $P_{S,0}$ as the polarization of the material, if it had 100 vol% of mesogenic sublayers.

$$\text{Vol}\,\%\,(\text{mesogen}) = \frac{V_{\text{mesogen}}}{V_{\text{total}}} \cdot 100 = \frac{d_{\text{mesogen}}}{d_{\text{total}}} \cdot 100, \tag{2}$$

$$P_S = \frac{P}{V_{\text{total}}} = P_{S,0} \cdot \frac{V_{\text{mesogen}}}{V_{\text{total}}}. \tag{3}$$

From figure 11 it seems that $P_{S,0}$ (proportional to the polarization per smectic sublayer) becomes constant for small vol per cent of mesogens. In this case the linear relationship should hold (see equation (3)). For systems with a higher concentration of mesogens, in which the mesogens are linked in close proximity to each other to the polymer chains, $P_{S,0}$ increases. Obviously the interactions of the mesogens—mediated by the polymer chain increase and lead to a higher polarization. It is interesting to note that the polarization of the monomer **7** also increases by polymerization, which leads to a density increase and thereby to stronger intermolecular interactions.

A typical measurement of the temperature dependence of the response time τ is shown in figure 12 for polymer **6d** for two different applied fields. Close to the transition ($T_c - T = 0{\cdot}5°C$), switching times as short as 600 μs were measured, whereas on cooling, due to the strong temperature dependence of the rotational

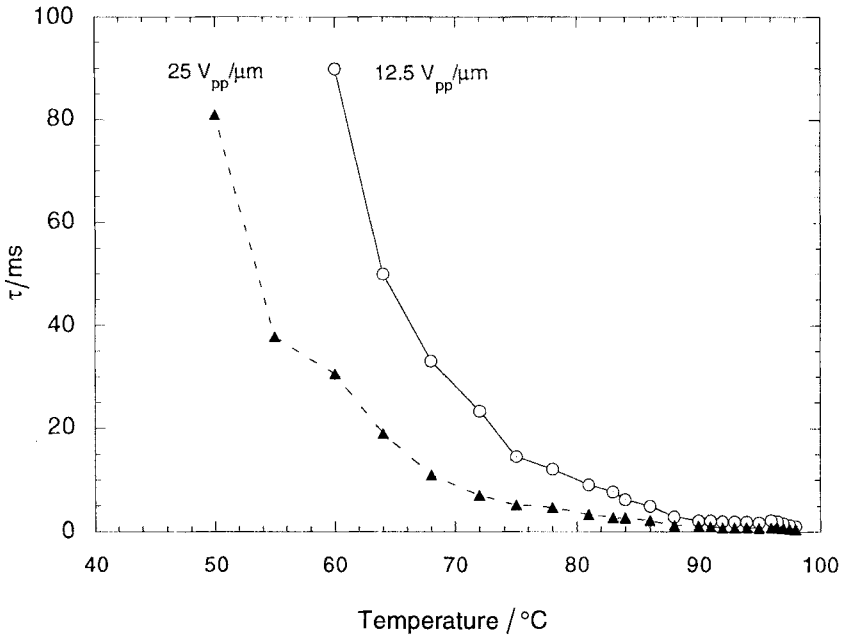

Figure 12. Optical response time τ (0–100 per cent) versus temperature for 12·5 and 25 $V_{pp}\,\mu m^{-1}$ for polysiloxane **6d**.

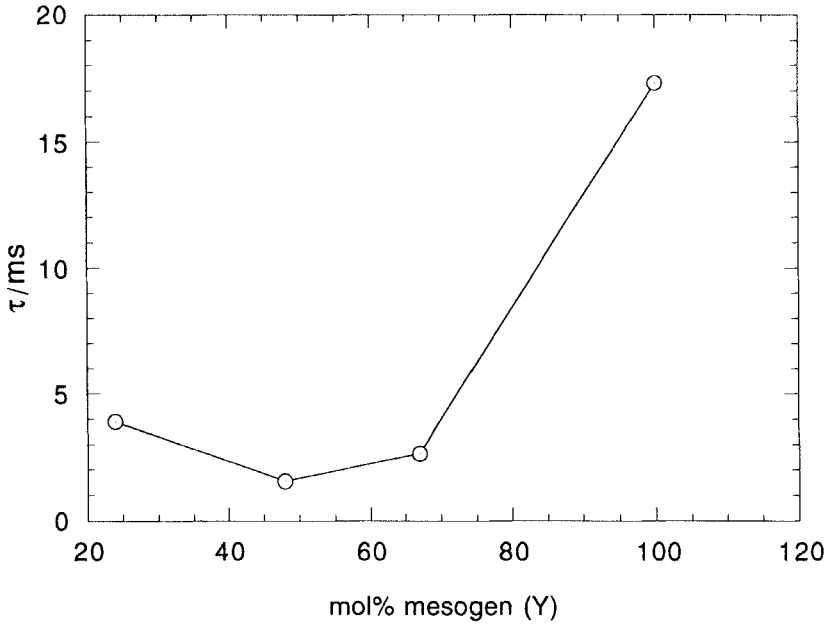

Figure 13. Optical response time τ (0–100 per cent) as a function of mol% of mesogen for polymers **6a–d** at $T_c - T = 10°C$.

viscosity γ, response times closer to 100 ms were reached. A τ versus reciprocal voltage plot reveals good linearity, but a clear deviation from the $\tau \sim E^{-1}$ law with a calculated exponent of $-1{\cdot}33$. By 'dilution', a noticeable fall (see figure 13) in the response times τ is observed for the polymers **6a–d**, which is due to the reduction of the rotational viscosity of the polymers by incorporation of non-mesogenic dimethylsiloxane units (DMS). Moreover, taking the $\tau \sim \gamma / P_S \cdot E$ law into consideration, the loss of the spontaneous polarization by 'dilution' has to be overcompensated by a decrease of γ in order to give faster response times τ. This result gives a further hint that 'dilution' of a FLC polysiloxane with non-mesogenic (isotropic) DMS-units seems to be a quite effective approach to reducing the switching times [20]. The increase of τ for the most 'diluted' polymer **6d** is not yet understood. Even if τ is corrected for the loss of P_S for the 'dilution' from **6c** to **6d**, the response time of **6d** is still longer than that for **6c**, indicating an increase in the rotational viscosity γ. Perhaps this is due to the fact that the transition temperature of the latter compound is higher and higher temperatures cause smaller rotational viscosities. So polysiloxane **6c**, with a substitution degree of 48 mol% of mesogenic side chains combines rather small viscosities with sufficiently high polarization in order to explain the short response times.

5. Experimental part

The infrared spectra were run on a 5DXC Nicolet FTIR spectrometer and the NMR spectra using Bruker 400 and 200 MHz FTNMR spectrometers. Specific rotations were measured with a Perkin–Elmer 141 polarimeter. Gel chromatographic measurements were made with a Waters Liquid Chromatograph equipped with a UV-Detector (254 nm) and a Data Modul 745 (Waters) using $CHCl_3$ or THF as solvents and against polystyrene standards.

Poly-(methylhydrogen)-siloxane ($P_n > 35$, E. Merck) **1a** and poly(methylhydrogen-co-dimethyl)-siloxane **1b–d** (copolymerization ratio: $Y:X = 1:0{\cdot}5$; $1:1{\cdot}1$; $1:2{\cdot}7$, $P_n > 30$, Wacker Chemie) were used as received. Toluene, used in the hydrosilylation reaction, was boiled over potassium and distilled under nitrogen. Commercially available chemical reagents and solvents were used directly without further purification, unless otherwise mentioned.

5.1. *Polysiloxanes **3a–d** with acetate protecting groups*

The precursor polymers **3a–d** with acetate protecting groups were synthesized by hydrosilylation of 4-(undec-10-enyloxy)-4′-acetoxybiphenyl **2** [9] with poly-(methylhydrogen)-siloxane **1a**, as well as with poly-(methylhydrogen-co-dimethyl)-siloxane **1b–d**, using dicyclopentadienylplatinium(II) chloride [25] in toluene. Typically 0·3–1·3 g (2·6–5 mmol) of the poly-(methylhydrogen)-siloxane **1a–d** and an excess (10 mol% relative to the Si–H groups) of 4-(undec-10-enyloxy)-4′-acetoxybiphenyl **2** were dissolved in 20 ml of potassium dried, freshly distilled toluene. The reaction flask was sealed with a septum and heated for 10 min at 80°C, while a stream of dry nitrogen was bubbled through the mixture with a cannula. After cooling to room temperature, 0·3–0·5 ml of a solution of dicyclopentadienylplatinium(II) chloride in toluene (2 mg/2 ml) was injected with a syringe. The septum was exchanged for a stopper and the reaction mixture was stirred at 90°C under a nitrogen atmosphere. After 24 h, the same amount of catalyst was injected once more and this procedure was repeated (3–5 d) until IR spectra revealed a disappearence of the Si–H-vibration at $\approx 2160\ cm^{-1}$. If this was not the case, a mop-up procedure [23] was used to remove all reactive binding-sites with a 10-fold excess of 1-octene, 0·2 ml of catalyst solution

and another 24 h period of reaction time. In polymer **3d**, a small number (< 15 per cent) of octyl groups were detected by ^{1}H NMR. In polymers **3a–c** no incorporation of octyl groups could be resolved, although a small Si–H signal (< 5 per cent) could still be detected. It seems possible that some of the poly-(methylhydrogen)-siloxanes **1a–d** are not fully linear, but partially branched. Purification of the polymers was effected by precipitation from methanol/acetone (1 : 1), subsequent centrifugation and drying in vacuo for 12 h at 40°C. To remove any traces of the catalyst, the crude polymers were dissolved in $CHCl_3$ and filtration through a short column filled with alumina oxide (neutral) was performed. The polymer solutions collected were filtered through a PTFE-filter (pore size = 0·25 μm), precipitated from methanol and dried after centrifugation in vacuo at 40°C for 12 h to give the cream coloured polymers **3a–d** in yields from 55–83 per cent. Molecular weights and phase transitions are in table 1.

3c: ^{1}H NMR ($CDCl_3$, 200 MHz): δ(ppm) = 7·39–7·49 [m, 4 $H_{arom.}$, $H_{2,2',6,6'}$-biphenyl, 7·05–7·09 [d, 2 $H_{arom.}$, $H_{3',5'}$-biphenyl, ^3J = 7·5 Hz], 6·87–6·91 [d, 2 $H_{arom.}$, $H_{3,5}$-biphenyl, ^3J = 7·5 Hz], 3·91 [m, 2 H, -CH_2–O–biphenyl], 2·27 [s, 3 H, CH_3–CO–], 1·72–1·74 [m, 2 H, –CH_2–CH_2–O–], 1·25–1·56 [m, 16 H, Si–$(CH_2)_8$–CH_2–], 0·48 [m, 2 H, Si–CH_2–], 0·05 [s, $(CH_3)_3$–Si–end groups], 0·02 [s, CH_3–Si– + $(CH_3)_2$–Si–O–]. IR (NaCl): ν (cm^{-1}) = 3041 (ν=C–H), 2961, 2921, 2853 (CH_2, CH_3), 1753 (ν C=O), 1608, 1572, 1527, 1498, 1472, 1435 (ν C=C), 1260, 1242 (ν C–O).

5.2. *Synthesis of polysiloxanes* ***4a–d***

The cleavage of the acetate protecting groups from polysiloxanes **3a–d** was done by hydrazinolysis using a modified literature method [9, 38]. As a typical example, the synthesis of polymer **4c** was as follows: To a solution of 0·8 g (1·6 mmol) of polymer **3c** in 300 ml of THF/dioxane (vol. ratio: 1 : 1) was added 2·57 g (41·2 mmol) of hydrazine hydrate (80 per cent by weight in H_2O) and the mixture was stirred overnight at room temperature. The milky reaction mixture was additionally boiled for 1 h. The absence of the C=O vibration ($\approx$1753 cm^{-1}) in the IR spectrum confirmed the completion of reaction. After cooling to room temperature, the polymer was precipitated from 800 ml of H_2O, separated by centrifugation or suction filtration and dried *in vacuo*. After a second precipitation from methanol, subsequent centrifugation and drying *in vacuo* at 40°C, pure polymer **4c** was obtained as a white–grey solid. Yield: 0·56 g (80 per cent).

4c: ^{1}H NMR (THF-d_8, 200 MHz): δ(ppm) = 8·28 [s, 1 H, biphenyl-OH] 7·31–7·41 [m, 4 $H_{arom.}$, $H_{2,2',6,6'}$-biphenyl], 6·84–6·88 [d, 2 $H_{arom.}$, $H_{3',5'}$-biphenyl, ^3J = 8 Hz], 6·73–6·77 [d, 2 $H_{arom.}$, $H_{3,5}$-biphenyl, ^3J = 8 Hz], 3·91 [m, 3 H, –CH_2–O-biphenyl], 1·72–1·74 [m, 2 H, –CH_2–CH_2–O–], 1·32–1·39 [m, 16 H, Si–$(CH_2)_8$–CH_2–], 0·58 [m, 2 H, Si–CH_2–], 0·1–0·0 [s, $(CH_3)_3$–Si-end groups, CH_3–Si- + $(CH_3)_2$–Si–O–]. IR (NaCl): ν(=cm^{-1}) 3280 (ν O–H); 2974, 2930, 2857 (CH_2, CH_3); 1610, 1501, 1461, 1450 (ν C=C); 1261, 1244 (ν C–O).

5.3. *Synthesis of the ferroelectric polysiloxanes* ***6a–d***

The ferroelectric polysiloxanes **6a–d** were synthesized by a polymer analogous reaction of the phenolic hydroxy groups of polymers **4a–d** with 3-nitro-4-((*S*)-1-methylheptyloxy)benzoic acid **5** according to Kapitza [9]. In a typical run 0·25 g (0·54 mmol) of polymer **4c**, 0·33 g (1·1 mmol) of 3-nitro-4-((*S*)-1-methylheptyloxy)benzoic acid **5** and a trace of 4-*N*,*N*-dimethylaminopyridine (DMAP) were suspended in 10 ml of a dry CH_2CH_2/THF mixture (1 : 1). The reaction mixture was

cooled under nitrogen in an ice bath, 0·23 g (1·1 mmol) of *N,N'*-dicyclohexylcarbodiimide (DCC) added, and stirred overnight. The urea was filtered off and the clear solution was twice put through a precipitation procedure using a methanol/acetone mixture (1 : 1) centrifuged and dried for 12 h at 40°C to give the pure polymer **6c**. Yield: 0·35 g (85 per cent). $[\alpha]_D = +3{\cdot}5°$ ($c = 0{\cdot}53$, $CHCl_3$).

6c: ^{1}H NMR ($CDCl_3$, 400 MHz): δ(ppm) = 8·59 [s, 1 H, H_2-nitrobenzoate], 8·27 [s, 1 H, H_6-nitrobenzoate], 7·45–7·54 [m, 4 $H_{arom.}$, $H_{2,2',6,6'}$-biphenyl], 7·11–7·19 [m, 3 H, $H_{3',5'}$-biphenyl, H_5-nitrobenzoate], 6·92 (b, 2 $H_{arom.}$, $H_{3,5}$-biphenyl], 4·61 [m, 1 H, O–C**H***–C_6H_{13}], 3·95 [m, 2 H, –CH_2–O-biphenyl], 1·72–1·74 [m, 2 H, –CH_2–CH_2–O–], 1·26–1·77 [m, 31 H, Si–$(CH_2)_9$–CH_2–, CH_3–CH*–$(CH_2)_5$–], 0·84–0·87 [t, 3 H, O–CH*–$(CH_2)_5$–CH_3], 0·49 [m, 2 H, Si–CH_2–], 0·05 [s, $(CH_3)_3$–Si-end groups], 0·02 [s, CH_3–Si– + $(CH_3)_2$–Si–O–]. IR (KBr): ν(cm^{-1}) = 3021 (ν=H), 2924, 2954 (CH_2, CH_3), 1757 (ν C=O), 1615, 1498, 1468, 1435 (ν C=C), 1536 (ν NO_2), 1351 (ν NO_2), 1260, 1211 (ν C–O).

5.4. *Synthesis of 4-(1-(R)-methylheptyloxy)-3-nitro-benzoic acid 4'-(undec-10-enyloxy)biphenyl-4-yl ester 7*

Preparation of the monomer **7** was done in a two step reaction starting from 4-(undec-10-enyloxy)-4'-acetoxybiphenyl [9], which was hydrolysed by NaOH/EtOH to give 4-(undec-10-enyloxy)-4'-hydroxybiphenyl. This was esterified with 3-nitro-4-(1-(*R*)-methylheptyloxy)benzoic acid **5** with *N,N*-dicyclohexylcarbodiimide (DCC) to yield the monomer **7**.

5.4.1. *4-(Undec-10-enyloxy)-4'-hydroxybiphenyl*

2·5 g (6·6 mmol) of 4-(undec-10-enyloxy)-4'-acetoxybiphenyl and 0·53 g (12·3 mmol) of sodium hydroxide were boiled for 6 h in 25 ml of ethanol/water (1 : 1). The solvent was evaporated, 100 ml H_2O were added and the solution was neutralized with hydrochloric acid (12 M). The precipitate was filtered off by suction filtration, dried *in vacuo* and recrystallized from ethanol. Yield: 1·4 g (64 per cent); m.p. = 145°C (dec.).

^{1}H NMR (DMSO-d_6, 200 MHz): 7·36–7·40 [d, 2 $H_{arom.}$, $H_{2,6}$, ^3J = 8 Hz], 7·19–7·23 [d, 2 $H_{arom.}$, $H_{2',6'}$, ^3J = 9 Hz], 6·85–6·89 [d, 2 $H_{arom.}$, $H_{3,5}$, ^3J = 8Hz], 6·56–6·60 [d, 2 $H_{arom.}$, $H_{3',5'}$, ^3J = 8 Hz], 5·67–5·84 [m, 1 H, CH_2=C**H**–], 4·88–4·94 [m, 2 H, **CH_2**=CH–], 3·89–3·95 [t, 2H, –**CH_2**–O–, ^3J = 6 Hz], 1·94–2·07 [m, 2 H, CH_2=CH–**CH_2**–], 1·61–1·71 [m, **CH_2**–CH_2–O–], 1·26–1·32 [m, 12 H, –CH_2–$(CH_2)_6$–CH_2–O–]. IR (KBr): ν(cm^{-1}) = 3380 (ν OH), 2921, 2854, (CH_2, CH_3), 1612, 1504 (ν C=C), 1269, 1266 (ν C–O). Elemental analysis: $C_{23}H_{30}O_2$ (338·49 g mol^{-1}): calculated C: 81·61, H: 8·94; found C: 79·95, H: 9·09 per cent.

5.4.2. *4-(1-(R)-methylheptyloxy)-3-nitro-benzoic acid 4'-(undec-10-enyloxy)-biphenyl-4-yl ester 7*

2·5 g (7·38 mmol) of 4-(undec-10-enyloxy)-4'-hydroxybiphenyl, 2·25 g (7·38 mmol) of 3-nitro-4-(1-(*R*)-methylheptyloxy)benzoic acid **5** and 50 mg of 4-*N,N'*-dimethylaminopyridine DMAP) were dissolved in 15 ml of dry CH_2Cl_2. After cooling the solution to 0°C, 1·67 g (8·1 mmol) of *N,N'*-dicyclohexylcarbodiimide (DCC) were added and the reaction mixture was stirred overnight at room temperature. The urea was filtered off and the solvent was evaporated. The residue was dissolved in ether and filtered again to remove urea. The solvent was evaporated and the remaining crude

product was purified by column chromatography on silica gel (60–100 mesh). Elution with $CHCl_3$ gave the pure product **7**, which was recrystallized from EtOH. Yield: 3·2 g (68 per cent); $[\alpha]_D = -2{\cdot}2°$ ($c = 0{\cdot}62$, $CHCl_3$); MS(FD): m/z (per cent) = 615·6 (MH^+, 100) ^{1}H NMR ($CDCl_3$, 200 MHz): δ(ppm) = 8·63–8·62 [d, 1 H, H_2-nitrobenzoate, $^4J = 2$ Hz], 8·29–8·34 [dd, 1 H, H_6-nitrobenzoate, $^3J = 9$ Hz, $^4J = 2$ Hz] 7·48–7·61 [m, 4 H, $H_{2,2',6,6'}$-biphenyl], 7·13–7·26 [m, $CDCl_3 + 3$ H, $H_{3',5'}$-biphenyl + H_5-nitrobenzoate], 6·94–6·99 [d, 2 H, $H_{3,5}$-biphenyl, $^3J = 8$ Hz], 5·71–5·91 [m, 1 H, CH_2=CH–], 4·90–5·04 [m, 2 H, CH_2=CH–], 4·59–4·68 [m, 1 H–CH*–$(CH_2)_5$–] 3·96–3·99 [t, 2 H, –CH_2–O–biphenyl, $^3J = 7$ Hz], 1·99–2·08 [m, 2 H, CH=CH_2–CH_2–], 1·31–1·83 [m, 27 H, –$(CH_2)_7$–CH_2–O, CH_3–CH*–$(CH_2)_5$–], 0·85–0·91 [t, 3 H, O–CH*–$(CH_2)_5$–CH_3]. IR (KBr): ν(cm^{-1}) = 2924, 2852, (CH_2, CH_3), 1740 (ν C=O), 1624, 1598 (ν C=C), 1538, 1350, (ν NO_2), 1288, 1248 (ν C–O). Elemental analysis: $C_{38}H_{48}O_6N_1$ (614·81 g mol^{-1}): calculated C: 74·11, H: 8·02, N: 2·27; found C: 74·15, H: 8·06, N: 2·17 per cent.

Financial support from Bundesministerium für Forschung und Technologie is greatly acknowledged. The authors would like to thank A, Nadler and B. Büchs for technical assistance and G. Henn (Max Planck Institut für Polymerforschung, Mainz) for helping to perform some of the X-ray measurements. Thanks as also due to Dr A. Schuster (Mainz) for computer programming.

References

[1] Clark, N. A., and Lagerwall, S. T., 1980, *Appl. Phys. Lett.*, **36,** 899.
[2] Lagerwall, S. T., Otterholm, B., and Skarp, K., 1987, *Molec. Crystals liq. Crystals*, **152,** 503.
[3] Escher, C., and Wingen, R., 1992, *Adv. Mater.*, **4,** 189.
[4] Shibaev, V. P., Kozlovsky, M. Z., Beresnev, L. A., Blinov, L. M., and Platé, N. A., 1984, *Polymer Bull.*, **12,** 299.
[5] Uchida, S., Morita, K., Miyoshi, K., Hashimoto, K., and Kawasaki, K., 1988, *Molec. Crystals liq. Crystals*, **155,** 93.
[6] Suzuki, T., Okawa, T., Ohnuma, T., and Sakon, Y., 1988, *Makromolek. Chem. rap. Commun.*, **9,** 755.
[7] Scherowsky, G., Schliwa, A., Springer, J., Kühnpast, K., and Trapp, W., 1989, *Liq. Crystals*, **5,** 1281.
[8] Dumon, M., Nguyen, H. T., Mauzac, M., Destrade, C., Achard, M. F., and Gasparoux, H., 1990, *Macromolecules*, **23,** 355.
[9] Kapitza, H., Zentel, R., Twieg, R. J., Nguyen, C., Vallerien, S. U., Kremer, F., and Wilson, C. G., 1990, *Adv. Mater.*, **4,** 792.
[10] Vallerien, S. U., Zentel, R., Kremer, F., Kapitza, H., and Fischer, E. W., 1989, *Makromolek. Chem. rap. Commun.*, **10,** 333.
[11] For a survey see: Special topic issue of ferroelectric polymers, 1992, *Polym. Adv. Tech.*, **3,** 195.
[12] Kapitza, H., and Zentel, R., 1988, *Makromolec. Chem.*, **189,** 1793.
[13] Coles, H. J., Gleeson, H. F., Scherowsky, G., and Schliwa, A., 1990, *Molec. Crystals liq. Crystals Lett.*, **7,** 125.
[14] Scherowsky, G., Beer, A., and Coles, H. J., 1991, *Liq Crystals*, **10,** 809.
[15] Vallerien, S. U., Kremer, F., Fischer, E. W., Kapitza, H., Zentel, R., and Poths, H., 1990, *Makromolek. Chem. rap. Commun.*, **11,** 593.
[16] Kapitza, H., Poths, H., and Zentel, R., 1991, *Makromolek. Chem., Makromolek. Symp.*, **44,** 117.
[17] Brehmer, M., Wiesemann, A., Zentel, R., Wagenblast, G., and Siemensmeyer, K., 1993, *Polprep. (Am. chem. Soc., Div. Polym. Chem.)*, **34,** 708.
[18] Hsu, C. H., and Percec, V., 1987, *Makromolec. Chem. rap. Commun.*, **8,** 331.
[19] Naciri, J., Pfeiffer, S., and Shashidar, R., 1991, *Liq. Crystals*, **10,** 585.

[20] DUMON, M., NGUYEN, H. T., MAUZAC, M., DESTRADE, C., and GASPAROUX, H., 1991, *Liq. Crystals*, **10**, 475.
[21] DECHER, G., REIBEL, J., HONIG, M., VOIGT-MARTIN, I. G., POTHS, H., ZENTEL, R., DITTRICH, A., and RINGSDORF, H., 1993, *Ber. Bunsenges. phys. Chem.*, **97**, 1386.
[22] GRAY, G. W., LACEY, D. NESTOR, G., and WHITE, M. S., 1986, *Makromolek. Chem. rap. Commun.*, **7**, 71.
[23] GRAY, G. W., HILL, J. S., and LACEY, D., 1990, *Makromolek. Chem.*, **191**, 2227.
[24] NESTOR, G., WHITE, M. S., GRAY, G. W., LACEY, D., and TOYNE, K. J., 1987, *Makromolek. Chem.*, **188**, 2759.
[25] APFEL, M. A., FINKELMANN, H., JANINI, G. M., LAUB, R. J., LÜHMANN, B.-H., PRICE, A., ROBERTS, W. L., SHAW, T. J., and SMITH, C. A., 1985, *Analyt. Chem.*, **57**, 651.
[26] POTHS, H., ZENTEL, R., VALLERIEN, S. U., and KREMER, F., 1991, *Molec. Crystals liq. Crystals*, **203**, 101.
[27] KAPITZA, H., and ZENTEL, R., 1991 *Makromolek. Chem.*, **192**, 1859.
[28] SKARP, K., ANDERSSON, G., LAGERWALL, S. T., KAPITZA, H., POTHS, H., and ZENTEL, R., 1991, *Ferroelectrics*, **122**, 127.
[29] POTHS, H., SCHÖNFELD, A., ZENTEL, R., KREMER, F., and SIEMENSMEYER, K., 1992, *Adv. Mater.*, **4**, 351.
[30] HONIG, M., GARBELLA, R. W., VOIGT-MARTIN, I. G., POTHS, H., and ZENTEL, R., 1993, *22. Freiburger Arbeitstagung Flüssigkristalle*, Freiburg, Germany.
[31] WALBA, D. M., RAZAVI, H. A., HORIUCHI, A., EIDMAN, K. F., OTTERHOLM, B., HALTIWANGER, R. C., CLARK, N. A., SHAO, R., PARMAR, D. S., WAND, M. D., and VOHRA, R. T., 1991, *Ferroelectrics*, **113**, 21.
[32] DIELE, S., OELSNER, S., KUSCHEL, F., HIGSEN, B., RINGSDORF, H., and ZENTEL, R., 1987, *Makromolek. Chem.*, **188**, 1993.
[33] WESTPHAL, S., DIELE, S., MÄDICKE, A., KUSCHEL, F., SCHLEIM, U., RÜHLMANN, K., HISGEN, B., and RINGSDORF, H., 1988, *Makromolek. Chem. rap. Commun.*, **9**, 498.
[34] KUSCHEL, F., MÄDICKE, A., DIELE, S., UTSCHICK, H., HISGEN, B., and RINGSDORF, H., 1990, *Polymer Bull.*, **23**, 373.
[35] MARTINOT-LAGARDE, P., 1977, *J. Phys., France*, **L-17**, 38.
[36] ESCHER, C., GEELHAAR, T., and BÖHM, E., 1988, *Liq. Crystals*, **3**, 469.
[37] POTHS, H., ZENTEL, R., ANDERSSON, G., and SKARP, K., 1992, *Adv. Mater.*, **4**, 791.
[38] CRIVELLO, J. V., DEPTOLLA, M., and RINGSDORF, H., 1988, *Liq. Crystals*, **3**, 235.